Spectral super-element approach to range-dependent ocean acoustic modeling

Henrik Schmidt, Woojae Seong [*], and Joo Thiam Goh
Department of Ocean Engineering, Massachusetts Institute of Technology, Cambridge, MA 02139.

(Received: ; Accepted for publication:)

The *spectral super-element* approach uses a hybridization of finite elements, boundary integrals, and wavenumber integration to solve the Helmholtz equation in a range-dependent ocean environment. The range-dependent ocean is divided into range independent sectors or *super-elements*. Wavenumber integral representations can be derived for an influence matrix representing the relation between displacement and pressure expansions on the vertical boundaries. The integration kernels are determined very efficiently by the Direct Global Matrix method in combination with a numerical quadrature scheme. The unknown expansion coefficients are then found by matching the boundary conditions of continuous displacement and stress between the sectors, with the acoustic field following by evaluating the wavenumber integrals within each sector, *e.g.* using the FFP technique. Two different boundary matching schemes are applied. One solves the global coupling problem incorporating all multiple scattering. A second, more efficient approach applies a single-scatter approximation at each vertical sector boundary, allowing for a marching solution. Numerical solutions to a series of canonical benchmark problems are given and compared to solutions obtained by other numerical approaches such as parabolic equations and coupled modes.

PACS numbers : 43.30Bp, 43.30Dr, 43.30Gv

INTRODUCTION

The last couple of decades has seen a significant effort in improving the numerical modeling capability for range-independent seismo-acoustic propagation and reverberation in the ocean environment [1].

The most general approaches are direct solutions of the wave equations using discrete methods such as the *finite difference methods* (FDM), and *finite element methods* (FEM). These methods rely on spatial and temporal discretizations which are small compared to the wavelengths in the problem, and since ocean acoustics problems are typically concerned with ranges of several hundreds or thousands of wavelengths, these discrete methods are in general prohibitive for computational reasons. As a result, the discrete methods are only important for modeling propagation and scattering in the near field.

Galerkin finite-element or *spectral methods* are used extensively in fluid dynamics [2] and to a limited degree in seismo-acoustic modeling [3]. These methods are in general well suited to wave propagation problems. The basis functions inherently possess some of the wave nature of the actual field, and the spectral methods therefore in general require less degrees of freedom than the discrete finite-element and -difference approaches. However, the computational savings are still insufficient for use of these methods for general long-range ocean waveguide problems.

Because of the computational limitations on the direct numerical solution of the wave equations, most modeling development and application in ocean seismo-acoustics has been centered around the classical modeling approaches, *ray tracing*, *parabolic equations*, *wavenumber integration*, and *normal modes* [1]. In addition to the computational issues, these methods are also usually preferred because of the fact that they provide frequency domain solutions. Due to the low cross-spectral coherence of long range ocean waveguide propagation frequency domain solutions are usually more relevant than the time domain solutions provided by most seismo-acoustic FEM and FDM algorithms.

Ray tracing remains a popular method due to its numerical efficiency, and the direct physical interpretation of the results. Further, it is well suited to handling range-dependence in two as well as three dimensions. However, ray theory provides a high-frequency approximation, and the associated limitations for seismo-acoustic modeling are well established. Also, ray tracing is not easily applied to propagation in elastic media because of the ray splitting associated with elastic conversion at interfaces.

The *parabolic equation* (PE) algorithm has undergone a dramatic development over the last couple of decades, and today is without doubt the most popular approach to seismo-acoustic modeling in range-dependent ocean waveguides. Even though the numerical solution is often performed using discrete methods such as FDM or FEM, the range discretization does not have to be smaller than a fraction of the wavelength. Also, the transformation into a parabolic equation allows for numerical solution using a marching scheme, and the PE is therefore in general ex-

[1]Present address: *Naval Arch. & Ocean Engg., Inha University, Inchon, Korea.*

tremely efficient compared to direct numerical solution of the eliptical Helmholtz equation. Due to the inherent one-way propagation assumption, the PE is limited to weak range dependence, but using a single-scatter approximation it has recently been extended to model backscattering [4]. Also, a PE for elastic propagation has recently been introduced [5]. As a result of these developments the PE is now applicable to most scenarios occuring in low to moderate frequency ocean seismo-acoustics. Compared to the other classical approaches a major drawback of the PE as well as the discrete methods is the fact that the solutions are not as easily interpreted physically. Thus, the modal structure of the field can only be determined through post-processing [6].

A common problem for all the classical, approximate aproaches, is the fact that the accuracy of the solution is not automatically guaranteed due to a dependency on computational parameters. However, this problem has traditionally been overcome by using two different modeling approaches. In that regard, extensive use of the elastic PE is hampered by a lack of other applicable modeling approaches. There is therefore a continuing effort being devoted to the development of the other classical modeling approaches to treat propagation and reverberation problems in a range-dependent ocean environment.

The wavenumber integration and normal mode approaches are based on integral transforms and therefore inherently limited to range-independent propagation problems. However, approximate solutions to range-dependent environments can be devised for both of these solution techniques.

Here, the adiabatic mode theory is well established and used extensively. However, due to the fact that it assumes that the mode shapes only undergo simple geometric scaling, the adiabatic approximation is restricted to weak range-dependence. Coupled-mode [7] algorithms have been developed which can handle strongly range dependent problems. The coupled mode approach is currently the primary provider of benchmark solutions, but existing implementations are limited to handling fluid waveguides only.

The wavenumber integration approach is the established benchmark for range-independent propagation in fluid-elastic waveguides [8], and a significant effort has been devoted to the development of an approximate extension to range-dependent environments. Lu and Felsen [9] derived an adiabatic transformation of the wavenumber integrals for weakly range-dependent problems. However, due to approximations made using dominant asymptotics, the method works well only for cases where the wave field is largely dominated by *discrete modes* [10]. Gilbert and Evans developed a one-way wavenumber integration approach for range-dependent fluid environments [11]. In contrast to the adiabatic approximation this approach handles full mode coupling, but the one-way approximation makes it applicable only to problems with weak contrasts in the range direction.

Wavenumber integration has been applied succesfully to range dependence which is limited in its horizontal extent, such as a finite size inhomogeneity in the seabed. By combining wavenumber integration with a boundary integral formulation for the scattered field, accurate solutions are obtained very efficiently for fluid as well as elastic environments [12, 13, 14, 15].

In the present *spectral super-element* method, the range-dependent ocean is divided into a series of range-independent sectors separated by vertical boundaries. In spite of some similarity to the traditional *spectral element* approach, there is a fundamental difference in terms of the horizontal dependence of the solution. In the spectral element approach this dependence is included in the degrees of freedom, whereas it is given explicitly in terms of a boundary integral in the present super-element approach. This is the key to the efficiency of the present approach to propagation in waveguides of long horizontal extent, prohibitive to traditional spectral element approaches.

The field in each sector or *super-element* is expressed as a superposition of that produced by any real source that might be present in the sector and the field produced by panel sources representing the discontinuities of the vertical boundaries. Since the super-element is horizontally stratified, the source field is given by a wavenumber integral, with the kernels determined very efficiently using the Direct Global Matrix (DGM) approach [16, 8]. The panel source contributions are expressed as a boundary integral which is changed to a discrete summation of influence functions by expanding the field along the vertical boundary in orthogonal polynomials. Using Legendre polynomials for the expansion, wavenumber integral representations for the influence functions are obtained. The kernels of these integrals are also evaluated very efficiently using DGM.

Since it does not rely on any wavelength-dependent discretization in the horizontal direction, the spectral super-element approach can be applied to short- as well as long-range propagation and reverberation problems. The wavenumber integration approach inherently decomposes the total solution into spectral components which is important for physical interpretations. The present method can also be extended in a straight forward manner to treat laterally inhomogeneous elastic media.

We describe two different solution algorithms. The first is a *global* approach, yielding both the forward propagating field and the back-scattered components. The coefficients are obtained from simultaneously matching the boundary conditions along all vertical sector boundaries. For ocean environments with continuously changing bathymetry, the construction and inversion of this matrix in a global manner presents a severe computational load. This deficiency has motivated the search for a more efficient formulation of the hybrid scheme. By employing the *single-scatter* approximation, where the back-scattered component from the opposite vertical boundary is neglected, a computationally efficient forward-marching scheme can be derived. We have also implemented a 2-way marching scheme providing a single-scatter approximation to the reverberation from large scale features, similar to the approach used in the two-way PE [4].

We would like to stress that the present approach should be considered a supplement rather than an alter-

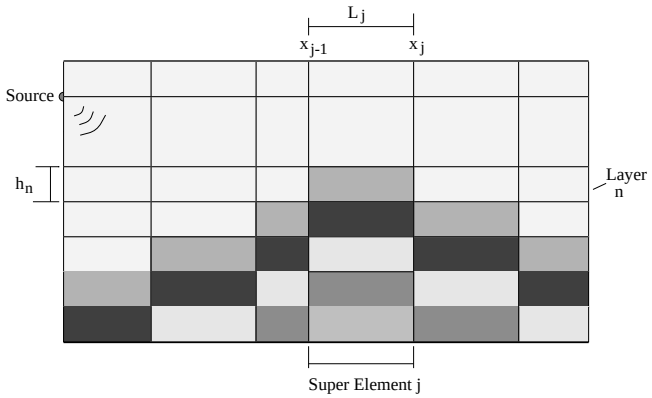

Figure 1: Super-element discretization of range-dependent ocean waveguides

native to other numerical approaches. Thus, it is ideally suited to canonical problems with few changes in bathymetry. It provides accurate solutions to problems with continuously changing bathymetry as well, but for such problems other methods such as the PE are in general more efficient. The main advantage of the present approach is the fact that the only approximation made is associated with the environmental discretization. There is no one-way assumptions made similar to those of the PE, and the numerical accuracy associated with the truncation of the expansion can be asserted by simple convergence analysis. As a result, the present approach can provide a *benchmark* for other more efficient approaches for problems with gradually changing bathymetry. Another advantage of the present approach is its conceptual validity for range-dependent fluid-elastic stratifications, as will be described in a future paper.

I. THE SPECTRAL SUPER-ELEMENT APPROACH

A. Stratified Super-Elements

In the *spectral super-element* approach , the environment is first divided into a series of range-independent *sectors* or *super-elements*, separated by vertical boundaries or *cuts*, as illustrated in Fig 1. The different grey-scales within each super-element denote layers with different material properties. Within each sector, the ocean environment is horizontally stratified. Here we will assume all layers to be fluid, but the approach is applicable to elastic stratifications as well. However, the additional algebra would obscure the fundamental principle of the approach, and we therefore limit ourselves to the fluid case in the present paper.

In deriving the spectral-element equations we will assume the acoustic field to be plane. Thus, in order to account for cylindrical spreading in axisymmetric scenarios, the spreading factor is applied explicitly to the resulting field. The validity of this approach is described in the appendix and an example of a numerical calculation is shown in Fig. (7).

Within each sector the acoustic pressure of time dependence $\exp i\omega t$ is given by

$$p(\mathbf{r}) = \rho\omega^2\phi(\mathbf{r}), \tag{1}$$

where ϕ is the displacement potential, satisfying the Helmholtz equation [1],

$$\left[\nabla^2 + k^2(\mathbf{r})\right]\phi(\mathbf{r}) = f(\mathbf{r})\ . \tag{2}$$

and $\mathbf{r}$ represents the spatial coordinates (x, z).

The field in sector j is now expressed as a superposition of the field produced in the stratified element in the absence of the vertical boundaries, ϕ^*, the field arising from the left boundary ϕ^-, and the field arising from the right boundary, ϕ^+,

$$\phi(x,z) = \phi^*(x,z) + \phi^-(x,z) + \phi^+(x,z) \tag{3}$$

The contributions $\phi^\pm$ from the vertical boundaries are determined using an *indirect* boundary integral method [17], based on Green's theorem for the virtual element obtained by eliminating the other vertical boundary and letting the element continue to infinity,

$$\begin{aligned}\phi^\pm(\mathbf{r}) \quad = \quad & \int_{S^\pm}\left[G(\mathbf{r},\mathbf{r}^\pm)\frac{\partial\phi^\pm(\mathbf{r}^\pm)}{\partial\mathbf{n}^\pm}\right. \\ & \left.-\phi^\pm(\mathbf{r}^\pm)\frac{\partial G(\mathbf{r},\mathbf{r}^\pm)}{\partial\mathbf{n}^\pm}\right]dS^\pm\ .\end{aligned} \tag{4}$$

Here $S^\pm$ is the boundary of the virtual elements. $G(\mathbf{r},\mathbf{r}^\pm)$ is an arbitrary Green's function satisfying the homogenous Helmholtz equation everywhere within the virtual element but not necessarily the boundary conditions. By choosing a Green's function which satisfies all boundary conditions at the horizontal interfaces, including the lower and upper boundaries of the super-element, then the contributions to the surface integral from the horizontal boundaries are eliminated. Note here, that the super-elements always have finite depth. Thus, in the presence of a lower halfspace, the lower boundary of the super-element is chosen deep enough into the halfspace to ensure that the field satisfies the radiation condition along the horizontal boundary, in which case the associated surface integral contribution vanishes. We would like to emphasize that this is different from the false bottom modal formulation of Evans [7] where the false bottom is introduced to achieve a complete mode set. In our approach, we only need to truncate the last layer at a depth where the dominant part of the field is downgoing.

If in addition we choose a Green's function which is symmetric in the horizontal coordinate x, $G(\mathbf{r},\mathbf{r}') = G(|x-x'|;z,z')$, then the term involving $\partial G/\partial\mathbf{n}^\pm$ in Eq. (4) will vanish, yielding

$$\phi^\pm(\mathbf{r}) = \int_{S^\pm} G(\mathbf{r},\mathbf{r}^\pm)\frac{\partial\phi^\pm(\mathbf{r}^\pm)}{\partial\mathbf{n}^\pm}dS^\pm\ , \tag{5}$$

B. Field Expansion

The boundary conditions to be satisfied between the super-elements, together with Eq. (5) now provides an integral equation for the field $\phi^\pm$ on the vertical boundaries of the super-element, the numerical solution of which

requires some kind of discretization. For fluid super-elements, the boundary conditions are the continuity of pressure and the horizontal component u of displacement, i.e. at the vertical boundary j separating super-elements j and $j+1$,

$$\left\{ \begin{array}{c} u(x_j,z) \\ p(x_j,z) \end{array} \right\}^j = \left\{ \begin{array}{c} u(x_j,z) \\ p(x_j,z) \end{array} \right\}^{j+1} \tag{6}$$

A superscript is used to identify the super-element here and in the following. Since the field within each layer in the stratification is a smooth function of depth, we here choose a *Galerkin boundary element* approach [1]. In the Galerkin approach, the continuity of the field across the vertical boundaries is expressed in the *weak form*

$$\int_0^{h_n} u^j(x_j,z)[u^{j+1}(x_j,z) - u^j(x_j,z)]dz = 0\,, \tag{7}$$

where z is the local depth coordinate and similarly for the pressure. The field parameters displacement and pressure are now expressed as expansions in terms of a set of basis functions. By choosing an orthogonal set of expansion functions Eq. (7) requires the expansion coefficients in the two neighboring sectors to be identical. Here we choose an orthonormal set of Legendre polynomials, normalized within each layer n:

$$\left\{ \begin{array}{c} u_n(x,z) \\ p_n(x,z) \end{array} \right\}^j = \frac{2\pi}{h_n} \sum_{m=1}^{\infty} \left\{ \begin{array}{c} U_{nm}(x) \\ S_{nm}(x) \end{array} \right\}^j P_{m-1}(\bar{z}) \tag{8}$$

where m is the order of expansion, P_m is the Legendre function and h_n is the thickness of layer n. The argument to the Legendre polynomial is the normalized, local depth coordinate

$$\bar{z}_n = \frac{z - h_n/2}{h_n/2}. \tag{9}$$

With the normal derivative of the displacement potential in the kernel of Eq. (5) representing the horizontal displacements at the vertical boundaries, insertion of Eq. (8) yields the following expression for the total field in super-element j

$$\begin{aligned} \phi(x,z) \;=\; & \sum_{l,k} F^j_{lk}(x - x_{j-1}, z) \left\{U^-_{lk}\right\}^j \\ & - F^j_{lk}(x_j - x, z) \left\{U^+_{lk}\right\}^j + \phi^*(x,z)\,. \end{aligned} \tag{10}$$

Here, $\{U^-_{lk}\}^j$ and $\{U^+_{lk}\}^j$ represent the unknown *panel source strengths* at the left and right boundary, respectively, of super-element number j, and

$$F^j_{lk}(x,z) = \frac{2\pi}{h_l} \int_{-1}^{1} P_{k-1}(\bar{z}'_l) G(x;z,\bar{z}'_l) d\bar{z}'_l\,. \tag{11}$$

Expanding the field parameters in Legendre polynomials within each layer n as in Eq. (8) then yields the following expression for the field expansion coefficients in terms of the unknown panel source strengths, $\{U^{\pm}_{lk}\}^j$

$$\begin{aligned} \left\{ \begin{array}{c} U_{nm}(x) \\ S_{nm}(x) \end{array} \right\}^j = & \left\{ \begin{array}{c} U^*_{nm}(x) \\ S^*_{nm}(x) \end{array} \right\}^j + \\ & \sum_{l,k} \left[\left\{ \begin{array}{c} C_{nm,lk}(x - x_j) \\ D_{nm,lk}(x - x_j) \end{array} \right\}^j \left\{U^-_{lk}\right\}^j \right. \\ & \left. - \left\{ \begin{array}{c} -C_{nm,lk}(x_{j+1} - x) \\ D_{nm,lk}(x_{j+1} - x) \end{array} \right\}^j \left\{U^+_{lk}\right\}^j \right]\,, \end{aligned} \tag{12}$$

and U^*_{nm} and S^*_{nm} are the expansion coefficients for the displacement and pressure produced by sources within the super-element. $C^j_{nm,lk}(x)$ and $D^j_{nm,lk}(x)$ are the expansion *influence functions* for displacement and pressure, respectively,

$$\begin{aligned} \left\{ \begin{array}{c} C_{nm,lk}(x) \\ D_{nm,lk}(x) \end{array} \right\}^j \;=\; & \frac{2m-1}{2\pi} \int_{-1}^{1} \left\{ \begin{array}{c} \partial/\partial x \\ \rho_n \omega^2 \end{array} \right\} F^j_{lk}(x,z) \\ & \times P_{m-1}(\bar{z}_n) d\bar{z}_n \end{aligned} \tag{13}$$

C. Influence Functions

It is clear from Eqs. (11) and (13) that the influence functions formally are obtained by a double depth-integral of the symmetric Green's function. However, using the direct global matrix (DGM) approach [16] we can replace these depth integrals by a wavenumber integral representation.

Basically the influence functions represent the expansion coefficients of order m in layer n produced by a *panel source* of order k in layer l. Thus, the total field is given as a superposition of the field $\hat{\phi}^{\pm}$ produced by the panel source in the absense of boundaries, and homogeneous solutions $\bar{\phi}^{\pm}$ accounting for interface reflections and transmissions [1]

$$\phi^{\pm}(x,z) = \hat{\phi}^{\pm}(x,z) + \bar{\phi}^{\pm}(x,z) \tag{14}$$

To determine the spectral representation of the field produced by the panel sources we use a generalization of the approach used by Heelan [18] for the constant stress panel. Thus, consider the panel source of order k in layer l, representing the displacement distribution

$$\hat{u}_l(x_{j-1},z) = \left\{ \begin{array}{ll} 0 & z < 0\,,\, z > h_l \\ \frac{2\pi}{h_l} P_{k-1}(\bar{z}_l) & 0 \le z \le h_l \end{array} \right. . \tag{15}$$

The displacement potential which satisfies the Helmholtz equation and the radiation condition can be written in terms of vertical wavenumber spectral representation as

$$\hat{\phi}_{lk}(x,z) \;=\; \int_{-\infty}^{\infty} \hat{A}_{lk}(\eta)\, e^{-x\gamma} e^{-i\eta(z - h_l/2)}\, d\eta \tag{16}$$

where η and $i\gamma = i\sqrt{\eta^2 - k_l^2}$ are the vertical and horizontal wavenumbers respectively and k_l is the acoustic wavenumber.

Differentiating Eq. (16) with respect to x to produce the horizontal displacement u, followed by the forward Fourier transform with respect to z gives

$$-\gamma \hat{A}_{lk}(\eta)\, e^{-x\gamma} e^{i\eta h_l/2} = \frac{1}{2\pi} \int_{-\infty}^{\infty} \hat{u}_l(x,z) e^{i\eta z}\, dz\,. \tag{17}$$

Substituting the boundary condition at $x = 0$, Eq. (15), and using the identity [19],

$$\int_0^{h_l} P_{k-1}(\bar{z}) e^{i\eta z} dz = h_l e^{i\eta h_l/2} i^{k-1} j_{k-1}(h_l\eta/2) \ , \quad (18)$$

the wavenumber kernel becomes

$$\hat{A}_{lk}(\eta) = -\frac{1}{\gamma} i^{k-1} j_{k-1}(h_l\eta/2) \ . \quad (19)$$

Note that the integration over z in the transform has been performed analytically and is accounted for by the spherical Bessel function j_{k-1}. Substitution into Eq. (16) yields

$$\hat{\phi}_{lk}(x,z) = -\frac{1}{\gamma} i^{k-1} \int_{-\infty}^{\infty} d\eta \ e^{-x\gamma} e^{-i\eta(z-h_l/2)} j_{k-1}(h_l\eta/2) , \quad (20)$$

which is the required free-space Green's function for the panel source in Eq. (15).

The DGM approach for the multi-layered sector requires the integral representation for the free-space Green's function to be expressed in terms of the horizontal wavenumber. Using contour integration as devised by Heelan [18], the vertical wavenumber integral of Eq. (20) is converted into a horizontal wavenumber integral,

$$\hat{\phi}_{lk}(x,z) = -i^{k-1} \int_{-\infty}^{\infty} ds \ \frac{1}{\alpha_l} j_{k-1}\left(-\frac{i\mathcal{S}h_l\alpha_l}{2}\right) e^{-|z-h_l/2|\alpha_l} e^{-isx} , \quad (21)$$

where s is the horizontal wavenumber, $\alpha_l = \sqrt{s^2 - k_l^2}$, and $\mathcal{S} = \text{sign}(z - h_l/2)$.

The above representation is valid only for $z \leq 0$ and $z \geq h_l$, but still allows for the application of the global matrix method when satisfying the horizontal interface boundary conditions since it is at the interfaces $z = 0$ and $z = h_l$ of each layer that the fields are being matched.

We now simply use Eq. (21) as the source contribution in the SAFARI code [8] to determine the associated homogeneous solution in layer n

$$\bar{\phi}_{n,lk}(x,z) = \int_{-\infty}^{\infty} \left[A^-_{n,lk} e^{-\alpha_n z} + A^+_{n,lk} e^{\alpha_n z}\right] e^{-isx} \ ds \ . \quad (22)$$

The influence functions are then obtained by expanding the total field in layer n in Legendre functions. The expansion of the homogeneous solution $\bar{\phi}_{n,lk}$ is performed directly using the identity in Eq. (18) to yield the homogeneous contribution to the influence functions:

$$\left\{ \begin{array}{c} \bar{C}_{nm,lk}(x) \\ \bar{D}_{nm,lk}(x) \end{array} \right\}^j = -(2m-1) i^{m-1} \int_{-\infty}^{\infty} \left\{ \begin{array}{c} is \\ \rho_n\omega^2 \end{array} \right\} \left[A^-_{n,lk}(s) + (-1)^{m-1} A^+_{n,lk}(s)\right] \times e^{-h_n\alpha_n/2} \ e^{-isx} \ j_{m-1}(ih_n\alpha_n/2) \ ds \ . \quad (23)$$

The corresponding direct contributions from the panel sources within the same layer are obtained by expanding the vertical wavenumber integral in Eq. (20) in Legendre functions, again using the identity in Eq. (18),

$$\left\{ \begin{array}{c} \hat{C}_{nm,lk}(x) \\ \hat{D}_{nm,lk}(x) \end{array} \right\}^j = \frac{\delta_{nl} h_n}{2\pi} \zeta_m \ i^{m+k-2} \int_{-\infty}^{\infty} d\eta \left\{ \begin{array}{c} 1 \\ \rho_n\omega^2/\gamma \end{array} \right\} e^{-x\gamma} \ j_{m-1}\left(\frac{h_n\eta}{2}\right) j_{k-1}\left(\frac{h_l\eta}{2}\right), \quad (24)$$

where δ_{nl} is the Kronecker delta and $\zeta_m = (2m-1)(-1)^{m-1}$. Each combination of indices l and k represents a single SAFARI run. However, the DGM can treat multiple right hand sides simultaneously. Hence, $A^{\pm}_{n,lk}$, and therefore all influence functions can be found using SAFARI for all combinations of the indices n, m, l, and k with just a single global matrix inversion. This makes the algorithm relatively efficient even for problems with a large number of layers and high orders of expansion.

D. Element Connectivity

Inserting the field expansions in Eq. (8) into the weak form of the boundary conditions in Eq. (7) leads to the *connectivity* equations between super-elements j and $j+1$,

$$\left\{ \begin{array}{c} U_{nm}(x_j) \\ S_{nm}(x_j) \end{array} \right\}^j = \left\{ \begin{array}{c} U_{nm}(x_j) \\ S_{nm}(x_j) \end{array} \right\}^{j+1} , \quad n = 1, \ldots N, \quad m = 1, \ldots M. \quad (25)$$

Here N is the number of layers, and M is the number of expansion terms used within each layer. Inserting Eq. (12) into Eq. (25) then yields the following linear system of equations for the unknown *panel source strengths* for super-elements j and $j+1$,

$$\sum_{l,k} \left[\left\{ \begin{array}{c} C_{nm,lk}(0) \\ D_{nm,lk}(0) \end{array} \right\}^{j+1} \{U^-_{lk}\}^{j+1} - \left\{ \begin{array}{c} -C_{nm,lk}(L_{j+1}) \\ D_{nm,lk}(L_{j+1}) \end{array} \right\}^{j+1} \{U^+_{lk}\}^{j+1} + \left\{ \begin{array}{c} -C_{nm,lk}(0) \\ D_{nm,lk}(0) \end{array} \right\}^{j} \{U^+_{lk}\}^{j} - \left\{ \begin{array}{c} C_{nm,lk}(L_j) \\ D_{nm,lk}(L_j) \end{array} \right\}^{j} \{U^-_{lk}\}^{j} \right] = \left\{ \begin{array}{c} U^*_{nm}(x_j) \\ S^*_{nm}(x_j) \end{array} \right\}^j - \left\{ \begin{array}{c} U^*_{nm}(x_j) \\ S^*_{nm}(x_j) \end{array} \right\}^{j+1} \quad (26)$$

Here, L_j is the horizontal length of the super-element. Solution of Eq. (26) yields the panel source strengths $\{U^{\pm}_{lk}\}^j$ in super-element j, and the resulting field is then given by Eq. (12), with the influence functions obtained through evaluation of the wavenumber integrals in Eqs. (23) and (24), using the FFP approach [1] and Gaussian quadrature, respectively.

II. NUMERICAL IMPLEMENTATION

A. Global Solution

In the *global* approach, the influence matrix for all sectors are computed to determine the coefficients in Eq. (26) which is then solved directly for all sector boundaries. This approach accounts for multiple scattering between sector boundaries. In order to set up this *global* influence matrix, the environment must be discretized such that the depth of each layer is the same for all sectors. In an ocean environment where the bathymetry changes continuously, such as a coastal wedge, a straight forward stair-case discretization of the bathymetry will require an excessively large number of layers. Here lies the greatest deficiency of the *global* approach.

B. Marching Algorithm

A computationally efficient forward marching scheme can be derived by employing the single-scatter approximation, where the back-scattered component from the forward vertical boundary is neglected. Thus, ignoring the term with $\{U_{lk}^{+}\}^{j+1}$ yields the following *marching* form of Eq. (26),

$$\sum_{l,k}\left[\left\{\begin{array}{c} C_{nm,lk}(0) \\ D_{nm,lk}(0) \end{array}\right\}^{j+1}\{U_{lk}^{-}\}^{j+1} + \left\{\begin{array}{c} -C_{nm,lk}(0) \\ D_{nm,lk}(0) \end{array}\right\}^{j}\{U_{lk}^{+}\}^{j}\right] = \left\{\begin{array}{c} U_{nm}^{*}(x_j) \\ S_{nm}^{*}(x_j) \end{array}\right\}^{j} - \left\{\begin{array}{c} U_{nm}^{*}(x_j) \\ S_{nm}^{*}(x_j) \end{array}\right\}^{j+1} + \left\{\begin{array}{c} C_{nm,lk}(L_j) \\ D_{nm,lk}(L_j) \end{array}\right\}^{j}\{U_{lk}^{-}\}^{j} \qquad (27)$$

After solving Eq. (27) at super-element boundary j, the field everywhere in the next sector follows from Eq. (12) with the backward propagating field ignored.

C. Reverberant Field

In the *global* approach, the forward and back scattered fields are computed simultaneously. Using an approach similar to the two-way PE solution [4], we can recover an approximation to the reverberant field from the *marching* solution as well. We start the forward solution at the source range and propagate the outgoing field across the range-independent sectors. At each vertical boundary, the influence matrix and the panel source strengths in the back-scattered direction are saved for later use. Starting at the maximum range, a back-scattered field is marched backwards towards the source. During this backward pass, the source strengths saved from the forward pass are added in. This process thus recovers the backscattered field in all the sectors.

III. NUMERICAL EXAMPLES

In the following we illustrate how the present approach provides accurate solutions to canonical propagation and reverberation benchmark problems. Unless otherwise stated, the water column is assumed to be homogeneous with a sound speed of 1500 m/s and density $\rho = 1.0\text{g/cm}^3$. As reference solutions, we use the FEPE [20] and COUPLE codes [7]. All our solutions are obtained using only four orders of expansion in the field parameters within each layer.

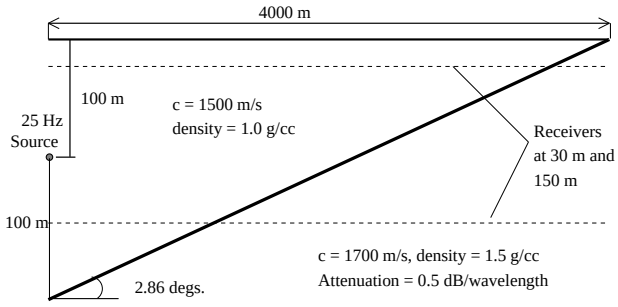

Figure 2: Schematic for the ASA benchmark problem (Ex. A).

Example A is the socalled ASA benchmark problem involving a cylindrically symmetric sloping ocean bottom [21]. The environmental model is shown in Fig. 2.This problem is considered to illustrate the accuracy of the outgoing field obtained using the marching algorithm. The water depth decreases linearly from 200m at $r = 0$ to zero at $r = 4$km. A 25-Hz point source is placed at mid-depth. In the homogeneous sediment, $c = 1700$ m/s, $\rho = 1.5\text{g/cm}^3$, and $\alpha = 0.5$ dB/λ. The backscattered field is negligible for this problem [22]. The environment is discretized into 17 layers, each of about a wavelength in depth, and 113 range sectors. The solutions for this problem appear in Fig. 3. The solid line is the solution obtained with the PE and the agreement is very good for the shallow receiver and satisfactory for the deeper receiver and for most practical purposes the differences can be considered as insignificant.

Example B involves a stair step in the ocean bottom with the ocean bottom acoustic parameters of example A. The water depth is a constant 200m for $r < 1.5$ km and 150 m for $r > 1.5$ km. A 25-Hz line source is placed at depth $z = 100$m. The abrupt change in the environment causes a significant amount of energy to be reflected from the stair face and into the water column. We solved this problem using only 2 range sectors and 8 layers down to a depth of 350m. Fig. 4 shows the environmental model and our solutions to the stair-step problem appear in Fig. 5. The super-element solution and the two-way coupled mode field are in excellent agreement. For this problem with only one vertical sector boundary, the global and marching schemes provide identical results.

Example C shown in Fig. 6 consider a seamount in a cylindrically symmetric ocean environment [11]. A 25 Hz source is located in the middle of the waveguide. The depth of the water column at the source range is 200 m. A 135 m high seamount has inner radius 5 km and outer radius 10 km. The bottom is a homogeneous half-space with a sound speed of 1700 m/s and density 1.5g/cm^3. The attenuation in the bottom is 0.5dB/λ. We solved this problem using only 3 range sectors and 8 layers down to a depth of 400m. Comparisons between COUPLE and our solutions are shown in Fig. 7.

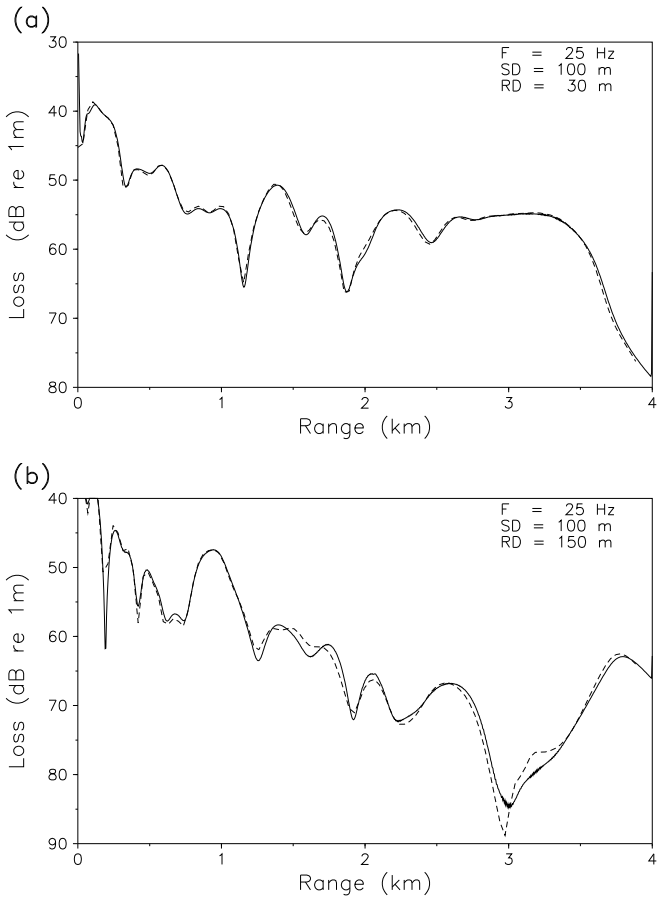

Figure 3: Solutions for example A. (a) Receiver at 30m, (b) Receiver at 150m: solid - PE; dashed - Spectral super-element solution.

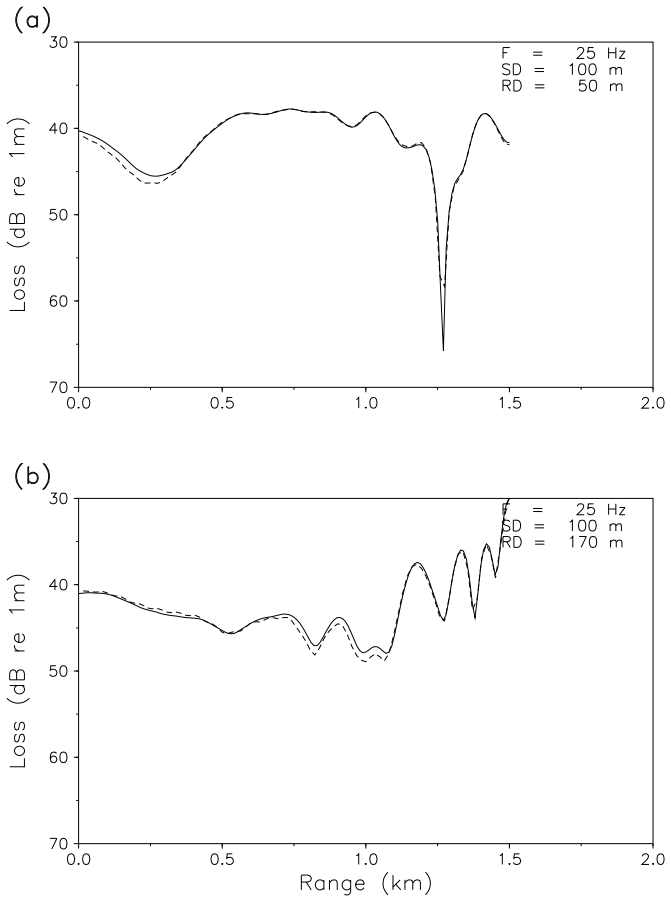

Figure 5: Backscattering from stair-step ridge (Ex. B). (a) Receiver at 50m, (b) Receiver at 170m: solid - COUPLE; dashed - Spectral super-element solution.

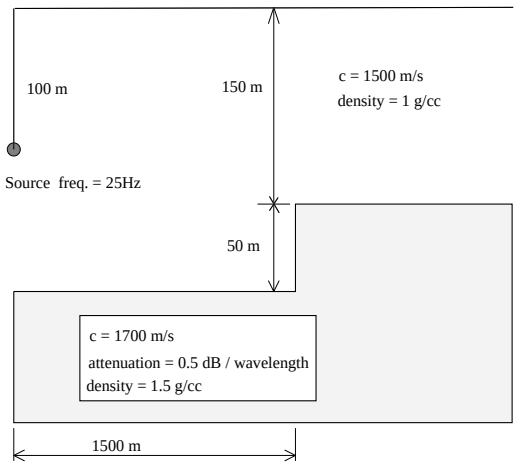

Figure 4: Schematic for the stair-step ridge problem (Ex. B).

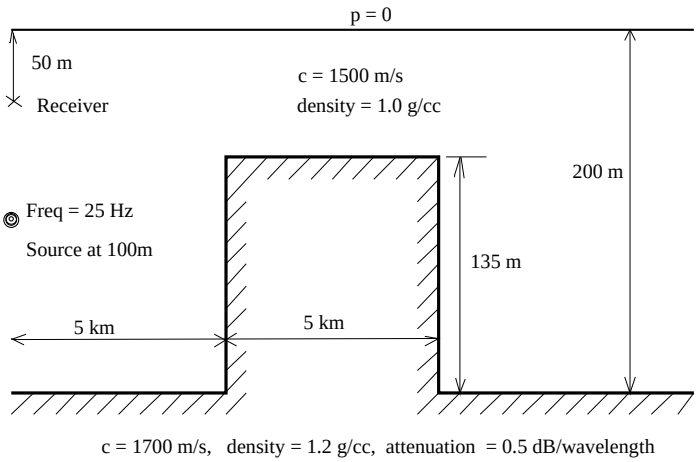

Figure 6: Schematic for the cylindrical seamount test problem (Ex. C).

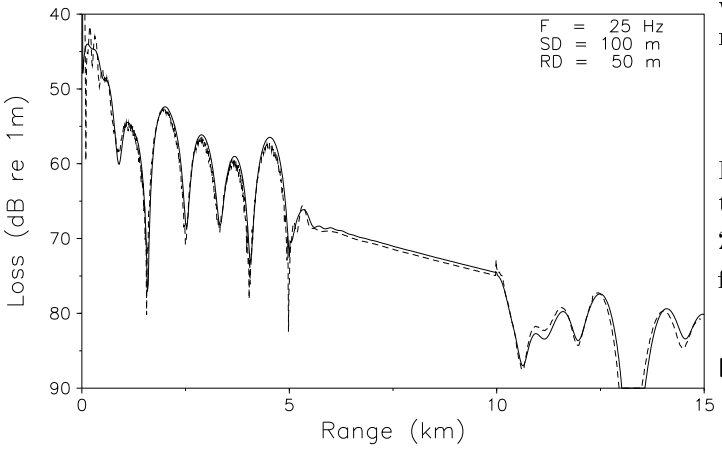

Figure 7: Cylindrical seamount (Ex. C). Receiver at 50m. solid - COUPLE; dashed - Spectral super-element solution.

IV. CONCLUSION

We have presented an efficient and versatile *spectral super-element* technique for wave propagation in multi-layered range dependent environments. The approach is capable of computing both the forward scattered and the reverberation field, and is particularly suitable for treating reverberation from large scale oceanic features and canonical benchmark problems. The numerical efficiency of the approach is obtained by using SAFARI to compute all influence functions for each super-element with one global matrix inversion. Wavenumber integration is also used for evaluating the field within each super-element once the boundary panel source strengths are found. By including a shear displacement potential and the associated additional boundary conditions at the vertical boundaries, the technique is straightforwardly extended to treat propagation in elastic media. Applications to canonical propagation and reverberation problems have been used to demonstrate the accuracy and versatility of the solution technique.

ACKNOWLEDGEMENTS

This work was supported by the Office of Naval Research, in part by the High Latitude Dynamics and the Ocean Acoustics programs.

APPENDIX: Axisymmetric environments

For cylindrical geometries, the Helmholtz reduced wave equation is

$$\frac{1}{r}\frac{\partial}{\partial r}\left(r\frac{\partial \Phi}{\partial r}\right) + \frac{\partial^2 \Phi}{\partial z^2} + h^2\Phi = 0 \ . \qquad (28)$$

We can separate out the cylindrical spreading effect by introducing

$$\phi(r,z) = \sqrt{\frac{\pi r}{2}}\Phi(r,z), \qquad (29)$$

where the coefficient is selected to give 0 dB loss at $r = 1$ m. Eq. (28) then becomes

$$\frac{\partial^2 \phi}{\partial r^2} + \frac{1}{4r^2}\phi + \frac{\partial^2 \phi}{\partial z^2} + h^2\phi = 0 \ . \qquad (30)$$

For large r_j, we may neglect the second term, and we see that cylindrical spreading can be treated with the present 2D derivation simply by including a factor of $\sqrt{\frac{2}{\pi r_j}}$ in the final evaluation of the field.

References

[1] F.B. Jensen, W.A. Kuperman, M.B. Porter, and H. Schmidt. *Computational Ocean Acoustics*. American Institute of Physics, Woodbury, NY, 1993.

[2] C. Canuto, M.Y. Hussaini, A. Quarteroni, and T.A. Zang. *Spectral Methods in Fluid Dynamics*. Springer Verlag, NY, 1988.

[3] E. Priolo, J.M. Carcione, and G. Seriani. Numerical simulation of interface waves by high-order spectral modeling techniques. *J. Acoust. Soc. Am.*, 95:681–693, 1994.

[4] M.D. Collins and R.B. Evans. A two-way parabolic equation for acoustic backscattering in the ocean. *J. Acoust. Soc. Am.*, 91 (3):1357–1368, 1992.

[5] M.D. Collins. An energy conserving parabolic equation for elastic media. *J. Acoust. Soc. Am.*, 94 (3):975–982, 1993.

[6] F.B. Jensen and H. Schmidt. Spectral decomposition of PE fields in a wedge-shaped ocean. In H.M. Merklinger, editor, *Progress in Underwater Acoustics*. Plenum Press, New York, 1987.

[7] R.B. Evans. A coupled mode solution for acoustic propagation in a waveguide with stepwise depth variations of a penetrable bottom. *J. Acoust. Soc. Am.*, 74:188–195, 1983.

[8] H. Schmidt. SAFARI: Seismo-acoustic fast field algorithm for range independent environments. User's guide. SR 113, SACLANT ASW Research Centre, La Spezia, Italy, 1987.

[9] I.T. Lu and L.B. Felsen. Adiabatic transforms for spectral analysis and synthesis of weakly range-dependent shallow ocean Green's functions. *J. Acoust. Soc. Am.*, 81:897–911, 1987.

[10] J.T. Goh and H. Schmidt. Validity of spectral theories for weakly range-dependent ocean environments - numerical results. *J. Acoust. Soc. Am.*, 95 (2):727–732, 1994.

[11] K.E. Gilbert and R.B. Evans. A Green's function method for one-way wave propagation in a range dependent ocean environment. In T. Akal and J.M. Berkson, editors, *Ocean Seismo-Acoustics*. Plenum Press, New York, 1986.

[12] G.T. Schuster and L.C. Smith. Modeling scatterers embedded in a plane-layered media by a hybrid Haskell-Thomson and boundary integral equation method. *J. Acoust. Soc. Am.*, 78:1387–1394, 1985.

[13] T.W. Dawson and J.A. Fawcett. A boundary integral equation method for acoustic scattering in a waveguide with nonplanar surfaces. *J. Acoust. Soc. Am.*, 87:1110–1125, 1990.

[14] P. Gerstoft and H. Schmidt. A boundary element approach to seismo-acoustic facet reverberation. *J. Acoust. Soc. Am.*, 89:1629–1642, 1991.

[15] M.W. Haartsen, M. Bouchon, and M.N. Toksöz. A study of seismic acoustic wave propagation through a laterally varying multilayered medium using the boundary-integral-equation-discrete-wavenumber method. *J. Acoust. Soc. Am.*, 96:3010–3021, 1994.

[16] H. Schmidt and G. Tango. Efficient global matrix approach to the computation of synthetic seismograms. *Geophys. J. R. Astr. Soc.*, 84:331–359, 1986.

[17] W. Seong. *Hybrid Galerkin boundary element - wavenumber integration method for acoustic propagation in laterally inhomogeneous media.* PhD thesis, Massachusetts Institute of Technology, January 1991.

[18] P.A. Heelan. Radiation from a cylindrical source of finite length. *Geophysics*, 18:685–696, 1953.

[19] I.S. Gradshteyn and I.M. Ryzhik. *Table of integrals, series and products.* Academic Press, 1980.

[20] Michael D. Collins. Benchmark calculations for higher-order parabolic equations. *J. Acoust. Soc. Am.*, 87:1535–1538, 1990.

[21] F.B. Jensen and C.M. Ferla. Numerical solutions of range-dependent benchmark problems in ocean acoustics. *J. Acoust. Soc. Am.*, 87:1499–1510, 1990.

[22] E.K. Westwood. Ray model solutions to the benchmark wedge problems. *J. Acoust. Soc. Am.*, 87:1539–1545, 1990.